Packed-Bed Reactor for Short Time Gas Phase Olefin Polymerization: Heat Transfer Study and Reactor Optimization

ARTICLE *in* AICHE JOURNAL · JANUARY 2012

Impact Factor: 2.75 · DOI: 10.1002/aic.12576

5 AUTHORS, INCLUDING:

Jean-Pierre Broyer
CPE Lyon
20 PUBLICATIONS **349** CITATIONS
SEE PROFILE

Timothy F.L. McKenna
Centre National de Recherche Scientifique, L…
215 PUBLICATIONS **2,548** CITATIONS
SEE PROFILE

Packed-Bed Reactor for Short Time Gas Phase Olefin Polymerization: Heat Transfer Study and Reactor Optimization

Estevan Tioni
Université de Lyon, Univ. Lyon 1, CPE Lyon, CNRS, UMR 5265 Laboratoire de Chimie Catalyse Polymères et Procédés (C2P2), LCPP team, Bat 308F, F-69616 Villeurbanne, France

Dutch Polymer Institute (DPI), 5600 AX Eindhoven, The Netherlands

Roger Spitz, J. P. Broyer, Vincent Monteil, and Timothy McKenna
Université de Lyon, Univ. Lyon 1, CPE Lyon, CNRS, UMR 5265 Laboratoire de Chimie Catalyse Polymères et Procédés (C2P2), LCPP team, Bat 308F, F-69616 Villeurbanne, France

DOI 10.1002/aic.12576
Published online in Wiley Online Library (wileyonlinelibrary.com).

A specially conceived packed-bed stopped flow minireactor (3 mL) suitable for short gas phase catalytic reactions has been used to study the start-up of ethylene homopolymerization with a supported metallocene catalyst. Focus has been put on the heat transfer characteristics of the supported catalysts and on understanding the relationship between the initial rate and the relative gas/particle velocities and the influence of particle parameters in the packed bed. We performed a comprehensive study on the influence of various physical parameters on the heat transfer regime at start up conditions. The catalyst activity as well as the polymer morphology is shown to be dependent on heat transfer regime. The knowledge thus obtained is applicable to industrial problems like catalyst injection in fluidized beds and helps preventing experimental artifacts due to overheating in following studies. © 2011 American Institute of Chemical Engineers *AIChE J,* 00: 000–000, 2011

Keywords: polyolefins, packed-bed reactor, heat transfer, start-up, gas phase polymerization

Introduction

The annual production of polyethylene (PE) and polypropylene (PP) on supported catalysts in gas phase processes is likely to be on the order of 50–60 million tons in 2010[1]; the economic importance of this type of production is obvious. What is less obvious is how to experimentally study the relationship between production of PE and PP in the gas phase and the evacuation of heat from the particle.[2]

The process by which the particles of supported catalyst are transformed from catalyst particles into growing polymer particles is understood from a qualitative point of view: once the virgin catalyst particles are injected into the reactor, monomer diffuses from the bulk phase and begins to react at the active sites on the surface of the catalyst support. The support is typically either silica or magnesium dichloride and has a high surface area and porosity that allow for the deposition of a large number of active sites

Correspondence concerning this article should be addressed to V. Monteil at monteil@lcpp.cpe.fr and T. McKenna at mckenna@cpe.fr.

throughout the structure. Polymer then quickly accumulates, generating pressure throughout the particle and provoking a fragmentation of the support. Once the fragmentation step is complete, the resulting particle (now referred to as a polymer particle) will continue to grow as long as monomer arrives at the active sites. If the reaction proceeds as it should, then one particle of catalyst will lead to the production of one particle of polymer. For a more in-depth discussion of the process of catalyst fragmentation and growth, the reader is referred to earlier works from our group as well as the references therein.[2,3]

It is well known that the morphology of growing polymer particles as well as the properties of nascent polymer evolve very quickly during the early instants of a polymerization.[4–11] This phase of the reaction can be crucial in ensuring adequate polymer properties, obtaining or maintaining stable reactor operation, preventing fines generation, and avoiding temperature excursions and catalyst deactivation. The risks of overheating of particles are highest during the early instants of the reaction given the highly exothermic nature of these polymerizations (heats of reaction on the order of 100 kJ/mol[12] and rates of reaction on the order of 5–35 kg of polymer per gram of catalyst per hour) found in industrial processes. This problem is even more pronounced in gas phase reactions (to which we will restrict our discussion in this article).

Some interesting results come from early research work done on gas phase catalytic olefin polymerization under industrial conditions.[13,14] Simulations have shown that particle overheating is likely during the initial instants of reaction in gas phase reactions for highly active catalysts, and especially for catalysts that are quickly activated. The extent of the temperature excursions is of course dependent on a number of parameters (catalyst activity and size and gas velocity).[15–23]

It is possible to avoid (or eliminate) some of the difficulties occasionally encountered during the early stages of polymerization by choosing conditions such that the initial moments of the reaction occur at rates slower than the potential maximum. This can be done by introducing a prepolymerization step, where the catalyst fragmentation step and initial period of the polymerization occur under milder conditions than in the main reaction,[15] or by designing the catalyst so that the activity profile builds up slowly in the main reactor over the course of several tens of seconds or minutes. Either way, it is still necessary to understand the relationship between the reaction conditions, the shape and porosity of the particle (in other words, its morphology) as well as the temperature in the early instants of reaction to optimize the development of catalysts for gas phase reactions. However, because of the nature of the reactor contents, the hydrodynamics inside a fluidized bed reactor or stirred powder bed reactors (the major types of polyolefin reactors used in commercial processes) can be very complex, making heat transfer difficult to study in a bench scale device.[24] In addition, the rapid reactions and sensitive nature of the catalyst make it difficult to study heat transfer even at the laboratory scale using standard reactors.

Nevertheless, some studies have looked at trying to experimentally evaluate the way in which heat is evacuated from growing particles. For instance, some workers[25] used a gas phase reactor consisting of an isolated cell equipped with a plate to deposit the individual catalyst particles, a digital camera and a microscope to observe the growing particles and an infrared thermal camera to measure real time single particle temperature evolution. They showed how a single particle can undergo temperature excursions up to 20°C under realistic polymerization conditions (up to 15 bar and 80°C) and they were able to relate particle properties (i.e. size) and catalyst preparation method to temperature and activity evolution in the first reaction minutes. Even if this technique was very flexible (quick and direct method to compare different catalysts in a single experiment), it had some weak points: the gas is stagnant (difficult comparison with a real fluidized bed), the catalyst particles are isolated (condition not verified in industry), and the contact between the particles and the underlying surface can significantly influence the evacuation of energy from the particle.

Stopped (or quenched) flow reactors appear to be an attractive route to circumvent some of the problems related to experimental investigation of these highly active systems. Such reactors are designed to perform very short polymerization reactions (even less than 1 s) by briefly contacting the catalyst and monomer, then rapidly and effectively killing the catalyst. They have been successfully applied in olefin polymerization research for the past few decades, but have mostly focused on attempting to identify kinetic parameters in slurry phase reactions.[5,6,26–28]

Recently, our group developed and built a special reactor to perform stopped flow catalytic polymerizations in gas phase under realistic conditions.[11] The first version of such reactor consisted in a 1-mL packed catalytic bed capable of working at high temperatures and moderate pressures (up to 90°C and 10 bars). For the first time, evolution of PE properties together with particle morphology produced by classic Ziegler-Natta (ZN) catalysts in gas phase was obtained.

The original design was improved to allow us to recover a larger quantity of polymer, to control the flow over the bed better, and to measure the gas temperature.[29] Using this reactor, it was shown that it is possible to develop a relationship between how the heat transfer rate is controlled (governed mainly by gas flow rate) and the start-up kinetics of the polymerization of ethylene on a supported metallocene catalyst. It has also been used to show how a variation in the gas phase thermal conductivity can alter consistently the temperature profiles in the reactor thus giving very different values of catalyst activity.[30]

Heat transfer from solid to gas in a catalytic packed-bed reactor has been discussed in a number of publications, but for obvious reasons not for the specific case of olefin polymerization.[31–38] The complexity of the subject is such that the choice of the most suitable equations to apply for the calculation of the particle-gas heat-transfer coefficient is still an open question, particularly for low particle Reynolds number (<10). The result is a number of different equations whose validity depends on packing characteristics and flow field.[39–43] A large number of these equations can be expressed in the following general from:

$$Nu = C + Re^{a}\, Pr^{b} \tag{1}$$

with "a" and "b" assuming positive values between 0 and 1.

Nusselt, Reynolds, and Prandtl numbers are defined as follows:

$$Nu = \frac{hD_p}{k_f} \tag{2}$$

$$Re = \frac{\rho_f V_s D_p}{\mu_f (1-\varepsilon)} \tag{3}$$

$$Pr = \frac{Cp_f \mu_f}{k_f} \tag{4}$$

where h is the heat-transfer coefficient between a particle and the surrounding medium, D_p is the particle (catalyst) diameter, k_f is the fluid thermal conductivity, ρ_f is the fluid density, V_s is the fluid superficial velocity (volumetric flow rate/cross-sectional area of the bed), μ_f is the fluid viscosity, ε is the bed porosity, and Cp_f is the fluid specific heat. Expressing the adimensional numbers in terms of the physical variables allows us to rewrite Eq. 1:

$$h \propto Cp_f^b \mu^{(b-a)} V_s^a D_p^{a-1} k_f^{1-b} \rho^a \tag{5}$$

Equation 5 shows the influence of physical and operating parameters on the particle/gas heat-transfer coefficient.

The parameters easily controllable in our system on a wide range are the thermal conductivity of the gas phase (k_f), its specific heat (Cp_f), the gas velocity (V_s), and the particle diameter (D_p).

Also important in determining the bed temperature is the quantity of heat evacuated from the solid phase by convection, which is also dependent on physical and operating parameters as is expressed in the following equation:

$$Q_{\text{transferred to the gas}} = v\rho_f Cp_f \int_0^{tr} (Tg_{out} - Tg_{in})dt \tag{6}$$

where v is the gas volumetric flow rate, t_r is the reaction time, and Tg_{out} and Tg_{in} the measured inlet and outlet gas temperatures, respectively.

The objective of this work is to investigate the relationship between heat transfer, relative gas-particle velocities, and the parameters mentioned above for relatively short times. We have chosen to work with the time interval 0.1–75 s as it is thought that this will be indicative of the critical period for particle breakup and potential loss of control of bed temperature in gas phase reactions. For this reason, it is necessary to use catalysts loadings of 10–100 mg in the bed depending on catalyst activity and reaction time if we aim to be able to collect enough polymer to perform some analyses of kinetics, molecular weight distribution, and eventually morphology (this latter aspect will be investigated in more details in a future publication). Of course, the difficulty with high catalyst loadings in a packed bed is that, given the highly exothermic nature of the reaction, the poor thermal properties of the continuous gas phase, and the packed-bed configuration of the reactor thermal runaway might occur[44,45] so care will be taken to avoid such problems as presented below.

Experimental Part

Generalities

Ethylene with minimum purity of 99.5% was purchased from Air Liquide (France) and was passed over purifying columns before use. Argon from Air Liquide (France) with minimum purity of 99.5% was used to keep the reaction environment free of oxygen. Helium purchased from Air Liquide (France) was used as received.

Reactor technology

The reactor (Figure 1) consists of an internal circular metal chamber with a diameter of 20 mm and a depth of 10 mm closed with a frittered metal cartridge (see Ref. 30 for more details). The chamber is filled with a mixture of seedbed and catalyst (1–15% catalyst w/w depending on seedbed and reaction time) in a glove box to avoid contamination of the contents, inserted into the external chamber, and then closed with the frittered metal lid. Gas enters through the hole in the bottom of the external chamber and leaves through a similar hole at the back of the metal lid.

Filters 3-mm thick with 13 μm pores are present at the inlet and at the outlet of the gas to assure the bed stability under the flow of gas and to prevent solids loss during the reaction. A metering valve is present on the outlet stream allowing the regulation of the gas flow rate inside the reactor. The entire assembly is then plunged into a water bath to ensure constant inlet gas and jacket wall temperatures. Thermocouples at the inlet and outlet of the reactor allow us to record the temperature rise of the gas phase as it flows through the bed. Pressure, temperature, and flow rate of the feed are controlled (Figure 2).

The reactor is equipped with three miniature solenoid valves (ASCO Joucomatic, France) controlled by a Programmable Logic Controller equipped with software (Crouzet, Millennium II+, France): one for the feed, one for the quenching gas (CO_2) and one for degassing. The minimum time between subsequent actions of the solenoid is 0.1 s. The Reynolds number for the reaction conditions treated in this study varies from 0.1 to 20. From the Ergun equation, the maximum calculated pressure drop with reaction conditions used in this study is of 30 mbar. This allows us to consider constant pressure along the bed. As a first approximation, the gas is supposed to be in plug flow conditions and superficial velocity constant along z-axis even if, due to the high ethylene consumption, this might not be entirely true for the first reaction instants.

Catalyst

A metallocene catalyst supported on silica was used for these experiments. The zirconocene complex ($EtInd_2ZrCl_2$) was used as received and supported over silica treated with methylaluminoxane. Details on the method of supporting the active sites can be found in previously published work.[30] To our knowledge, this is the first study concerning metallocene supported catalysts at very short reaction times.

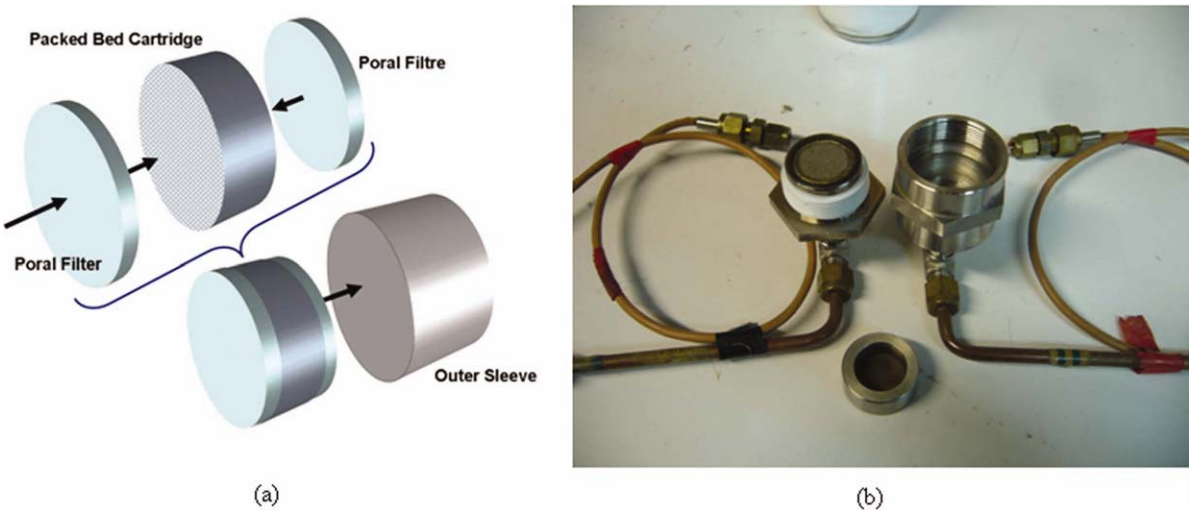

Figure 1. (a) Packed bed schematic view and (b) reactor photograph.

[Color figure can be viewed in the online issue, which is available at wileyonlinelibrary.com.]

Inert seedbed

The catalyst particles have to be highly diluted with inert solids in this type of reactor to ensure good control of the reaction temperature by reducing the quantity of heat produced per unit volume of bed.[11,29,30] In these previous studies, triethylaluminium (TEA)-treated silica was used as the inert diluent. This implies that solid liquid extraction is necessary to recover the polymer for analysis. The task can be particularly hard and tedious when dealing with very short reaction times, where the weight ratio of polymer/silica can be as low as 0.01. In addition, if one would like to observe the particles under Scanning Electron Microscopy (SEM) or other microscopy techniques, it will be difficult, especially for reactions where the catalyst has not fragmented yet, to distinguish catalyst particles (supported on silica) from inert bed particles. For these reasons, the seedbed used in this work was prepared from commercially available NaCl particles: the cubic form of NaCl crystals makes them easily recognizable in microscopy and a simple and elegant operating way to recover the catalyst/polymer particles for analysis is to wash the bed with demineralized water.

NaCl (Laurylab, France) was treated in different ways according to the desired application and used as seedbed. Large particle seed beds with a relatively narrow distribution were prepared by sieving the original salt to obtain a cut between 250 μm and 500 μm. To obtain seedbeds with small particle diameter, the salt was dissolved and crystallized in a controlled way[46] to obtain single crystals of 5 μm. According to this method, 450 mL of NaCl saturated water solution was added in one shot to 900 mL of 0.06 M solution of citric acid in ethanol. Citric acid avoids excessive agglomeration of the crystals. NaCl precipitates immediately at the contact with the antisolvent and the solution became milky. The resulting suspension was stirred for 60 min at 370 rpm and the NaCl was recovered and washed with ethanol to

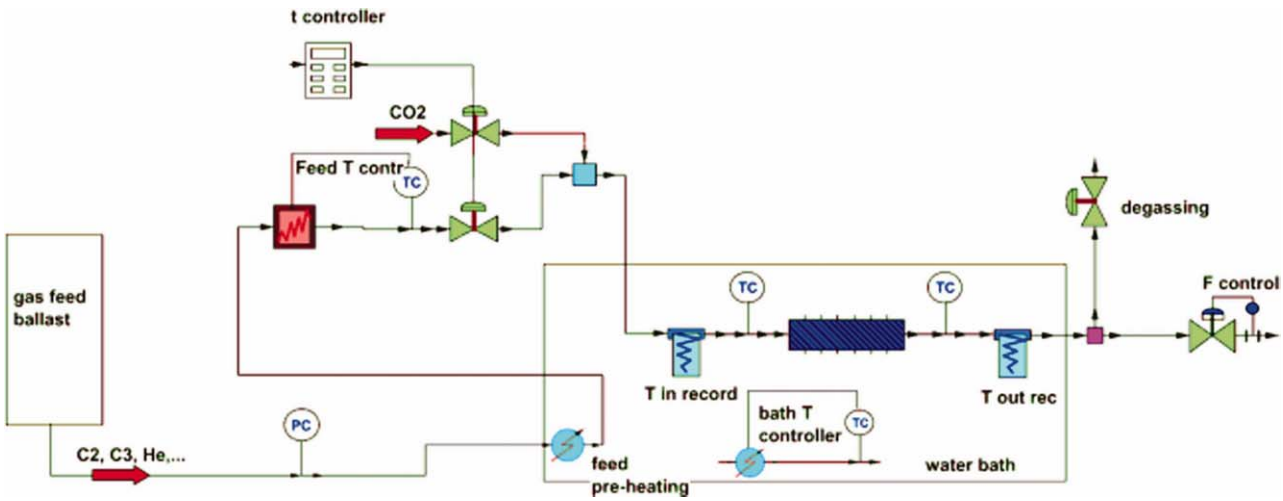

Figure 2. Schematic view of the reactor and control system.

[Color figure can be viewed in the online issue, which is available at wileyonlinelibrary.com.]

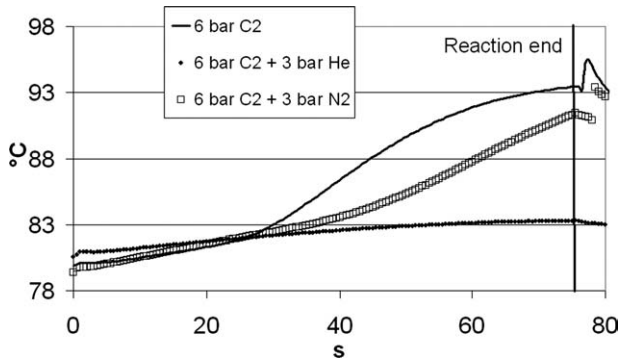

Figure 3. Effect of inert gas addition on outlet stream temperature (T = 80°C, P_{C2} = 6 bar, gas velocity = 3.0 cm/s, reaction time = 75 s, m_{cat} = 30 mg, seedbed = NaCl coarse).

eliminate the remaining water. The solid was dried for 2 h at 100°C and finally sieved. The fraction smaller than 45 μm was retained and dried for 4 h at 200°C to remove any trace of adsorbed water before use. The final solid consists of single cubes of 5–10 μm slightly agglomerated to give a final single object of around 30 μm.

All the inert seedbeds were dried under vacuum at 200°C for 4 h to remove the adsorbed water molecules before mixing with active catalyst.

Polymerization procedure

A typical polymerization is conducted as follows: initially, the reactor is filled with a mixture of seedbed and catalyst in a glove box, then it is connected to the feed line, plunged into the water bath, and swept with argon during the heating step. Once the working temperature is reached, the argon flow is stopped and then the feed solenoid is opened to allow the feed mixture to flow through the catalytic bed. After a predetermined time (varying from 0.1 s to 75 s), the quenching solenoid valve is opened and CO_2 flows through the catalytic bed removing the residual monomer and partially "killing" the catalyst. At the same time, the degassing solenoid valve is opened and the feed one is closed. This allows complete removal of residual reacting monomer even from the catalyst smaller pores thus stopping immediately the reaction.

Productivities are measured by weighing the reactor before and after the polymerization step in a glove box (after a drying period to ensure that there is no residual water on the reactor assembly). The polymer is recovered from the fixed bed after three washing steps: one with demineralized water followed by one with a solution of 10% w/w of HCl in demineralized water and finally one with pure demineralized water again. The polymer recovered is then dried under vacuum at 80°C for at least 1 h to eliminate the last traces of water.

SEM imaging

Morphology of the produced polymer particles was observed with scanning electron microscopy without separation from seedbed particles. Particle morphology images were recorded using a S800 Hitachi microscope (SEM) (CTμ, UCBL I, France) operating at accelerating voltages of 10 or 15 keV (depending on each individual case). As the catalyst we used (and especially its morphology) is highly sensitive to moisture, it is essential to carry out SEM observations under inert conditions.

Results and Discussion

Influence of gas thermal conductivity on heat transfer

In a previous paper,[30] it was shown that increasing the gas conductivity by using helium as a carrier gas rather than using nitrogen prevents bed overheating and polymer melting. The reactions in the previously presented work were performed at 80°C, 6 bar of monomer pressure, 3.0 cm/s gas velocity, coarse NaCl as seedbed, 30 mg catalyst, 75 s reaction time, and the evolution of the outlet gas phase temperatures are summarized in Figure 3, and the yield (Y) is shown in Figure 4. It can be seen from these figures that the use of helium as a carrier gas has two visible effects: (1) the outlet stream gas temperature is much lower in the case where helium was used as a carrier gas (Figure 3); and (2) it provokes a strong decrease on the yield (Figure 4). These changes are not caused by the dilution of the reacting monomer in the particle pores due to presence of helium since higher temperatures and yields are seen for the case of nitrogen as a carrier. Rather it appears that thermal conductivity increase when He is used as opposed to ethylene alone or ethylene plus N_2 leads to a better evacuation of the heat of reaction in the first case, and therefore a lower particle temperature than in the other two cases.

Thermal conductivity of helium is in fact almost 10 times higher than that of ethylene or nitrogen (0.172 W/m/K for helium, 0.0236 W/m/K for ethylene, and 0.0226 W/m/K for Nitrogen at 20°C and 1 atm).[47] As these polymerizations are exothermic, the lower temperature leads to a lower yield. This conclusion is also supported by the observation that when helium is in the feed a free flowing bed is recovered after the reaction. If no helium was mixed to the feed at least the central part of the bed was a solid block and only a small external annular section was a free flowing powder.

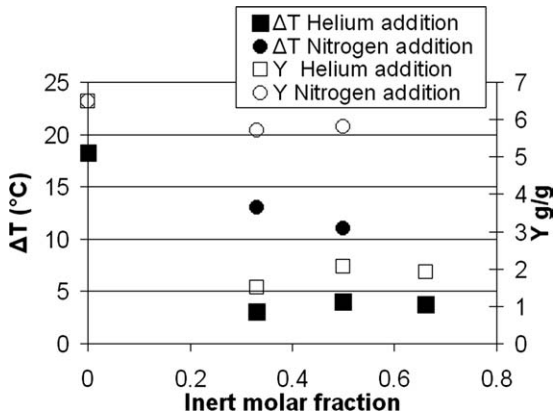

Figure 4. Influence of inert gas addition on yield and outlet gas temperature (T = 80°C, P_{C2} = 6 bar, gas velocity = 3.0 cm/s, reaction time = 75 s, m_{cat} = 30 mg, seedbed = NaCl coarse).[30]

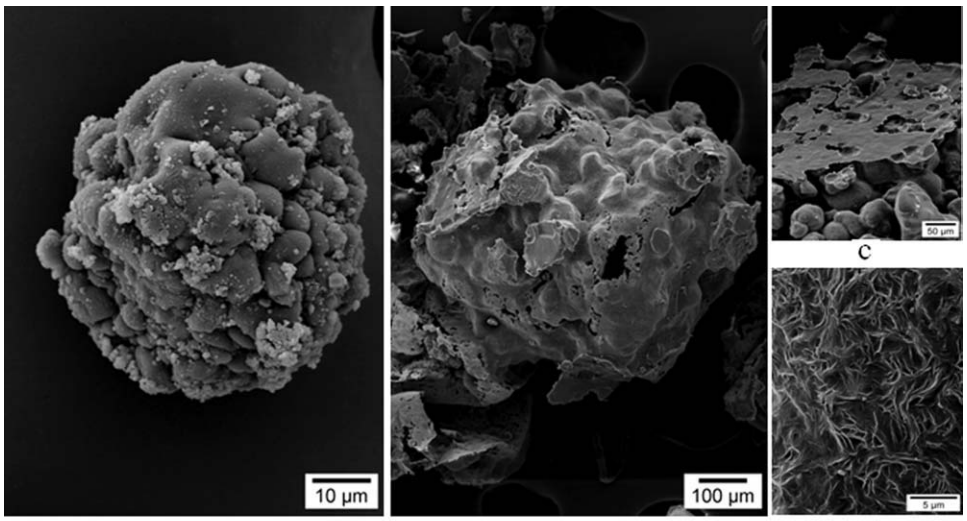

Figure 5. (a) Particle produced with addition of 0.67 helium molar fraction in the feed, (b) particle produced without addition of helium, (c) zoom on melted particle produced without helium addition: the flat surface is the footprint of a side of a NaCl grain, and (d) zoom of (b).

This is caused by an excessive temperature in the bed provoking PE melting (T_m around 130°C) and bed sintering.

In Figure 5, SEM pictures of polymer particles produced with (a) or without (b–d) addition of helium to the feed are represented. It is clear how the particles are spherical in the case when helium is used, whereas agglomerated and irregular particles showing signs of polymer melting and NaCl crystals footprint are visible when no helium is used in the gas stream.

High gas conductivity has the merit of improving the heat transfer from solid to gas and avoids particle overheating and thermal runaway of the reaction. Heat-transfer coefficient is in fact proportional to the fluid thermal conductivity and specific heat. Adding helium to the ethylene feed increases both values of these properties.

By using the Wassiljewa-Mason–Saxena method, it is possible to calculate the thermal conductivity of a gas mixture according to the following equation[48]:

$$k_{\mathrm{mix}} = \sum_i \frac{k_i y_i}{\sum_j A_{ij} y_i} \tag{7}$$

where y_i is the molar fraction of the ith component of the mixture, k_i is the thermal conductivity of the pure ith component, and A_{ij} are mixing parameters accounting enthalpy and entropic effects due to intermolecular interactions defined as follows:

$$A_{ij} = \frac{\left[1 + \left[\frac{\eta_i}{\eta_j}\right]^{0.5} \left(\frac{M_j}{M_i}\right)^{0.25}\right]^2}{\left[8\left(1 + \frac{M_i}{M_j}\right)\right]^{0.5}} \tag{8}$$

where η_i is the viscosity of the pure ith component and M_i its molecular weight. The viscosity and thermal conductivity of the pure components are calculated according to the Stiel–Thodos equations.[47]

To evaluate if the improvement in heat transfer is really due to a fluid thermal conductivity increase caused by helium, we used the simple Ranz-Marshall equation to calculate an approximate value of h, the gas solid heat-transfer coefficient, for different gas compositions. We used an average value of 50 μm for the catalyst particle diameter and a gas velocity of 3.0 cm/s. Table 1 shows how the gas properties and the a dimensional numbers vary with varying helium mole fraction in the mixture. Specific heats of pure compounds are calculated using the formulas proposed in Ref. 42. Density and specific heat of the mixture are calculated using the ideal gas mixing rule. Viscosity of gaseous mixture is calculated with the same mixing rule used for thermal conductivity.

It is clear that helium addition to the feed increases mainly the thermal conductivity of the mixture and the heat-transfer coefficient. For example, adding 3 bars of helium to the ethylene feed increases by a factor of 3 the heat-transfer coefficient. In addition, the increase of the specific heat of the gaseous mixture and of the mass flow rate of the gas phase provoked by an addition of helium in the feed (increased total pressure) leads to an augmentation of the quantity of heat evacuated from the solid phase by convection as is expressed in Eq. 6.

Table 1. Physical Properties of the Gaseous Mixtures (T = 80°C, P_{C2} = 6 bar)

y_{He} (Molar Fraction)	k_{mix} (W/m/K)	Cp_{mix} (J/kg/K)	η_{mix} (cP)	Nu	h (W/m^2/K)
0	0.0078	2087	0.0118	2.75	429
0.33	0.026	2294	0.0129	2.42	1262
0.50	0.041	2476	0.0136	2.34	1874
0.66	0.059	2778	0.0145	2.29	2754

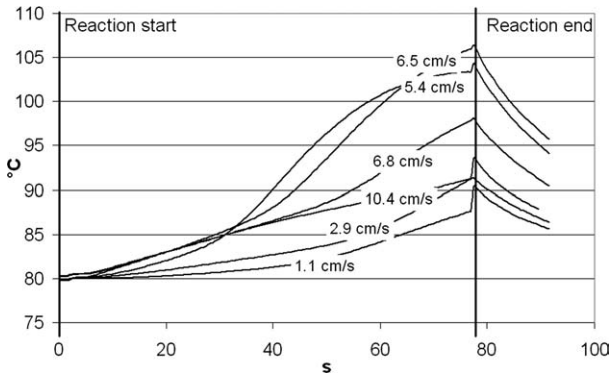

Figure 6. Outlet stream temperature profile at different gas flow rates without helium (series A: T = 80°C, P_{C2} = 6 bar, reaction time = 75 s, m_{cat} = 15 mg, seedbed = NaCl coarse).

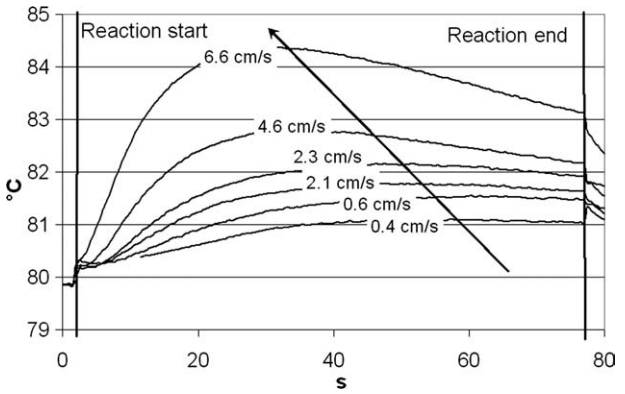

Figure 8. Outlet stream temperature profile at different gas flow rates in presence of helium: (T = 80°C, P_{C2} = 6 bar, P_{He} = 3 bar, reaction time = 75 s, m_{cat} = 30 mg, seedbed = NaCl coarse).

Influence of gas velocity on heat transfer

It is however clear that the gas velocity will also have an impact on the heat removal rate from the particles. To show that this set-up can also be used to explore the role of relative gas-particle velocities on particle heat removal (and thus on particle temperature), a number of different experiments have been performed with gas flowing at different superficial velocities on a bed of coarse NaCl particles (250–500 μm). The reactions were conducted for 75 s at a monomer relative partial pressure of 6 bars with eventual addition of 3 bars of helium and at 80°C.

Two series of experiments with varying gas velocity are presented in this section: one series (A) corresponding to poor heat transfer conditions (low gas thermal conductivity) and one (B) corresponding to improved heat transfer conditions (higher gas conductivity by helium addition). It is interesting to study the effect of the relative solid gas velocity for both experimental conditions on the thermal behavior of our packed bed.

The results of the runs in series A show that increasing the gas velocity through the bed up to about 6 cm/s leads to a higher outlet gas temperature (Figure 6) and to slightly lower yields (Figure 7). Beyond 6 cm/s, the maximum temperature (still at 75 s) of the outlet gas decreases then levels off. This implies that, at least in the range of velocity considered here, at low velocities the particles overheat and the gas–solid heat-transfer coefficient is too low to remove all the heat. As the velocity increases, the heat-transfer coefficient obviously increases as well. It appears that as h increases, the particles overheat less and this leads to a drop in the temperature of the polymerizing particles and thus the gas temperature. As these reactions are exothermic, lower temperature means slower rate. The lower rate gives lower yields and less heat being generated. This further suggests that the gas temperature at the outlet begins to approach that of the surface of the particles in the bed at a sufficiently high flow rate through the bed. In other words by maintaining an appropriately high flow rate, we can get an estimate of the actual surface temperature of the particles and therefore begin to quantify the relationship between the reaction rate and the temperature of the nascent particles.

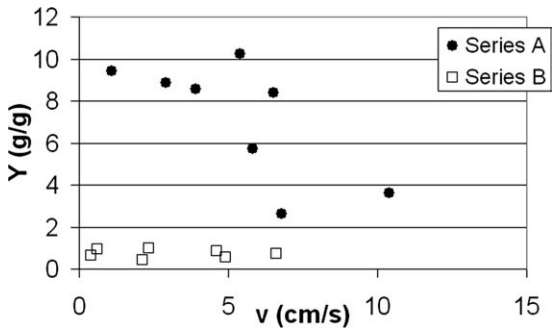

Figure 7. Yield dependence on gas velocity in absence (Series A) or presence (Series B) of helium: (T = 80°C, P_{C2} = 6 bar, (P_{He} = 3 bar), reaction time = 75 s, m_{cat} = 15 (series A) or 30 (series B) mg, seedbed = NaCl coarse).

Changing the relative gas–particle velocities in the presence of He (series B) leads to slightly different conclusions. As we saw above, using a carrier gas with a high thermal conductivity can itself help to avoid hotspots and thermal runaway. The combination of this with an increased flow rate has the effect of reducing the overheating of the particles and lowering the difference between the gas and the solid surface temperatures. Increasing the gas velocity provokes an increased outlet gas temperature (Figure 8), whereas yield stays constant (Figure 7). This is clearly an indication that higher quantities of heat are transferred to the gas flowing with an increased velocity. It can also be seen from Figure 8 that as the gas flow rate increases the maximum temperature at the outlet is observed earlier and earlier in the experiment. This phenomenon is not seen if pure ethylene is used in the feed stream (Figure 6).

Calculations of the total amount of heat transferred to the gas respect to the heat produced supports the results shown above (Figure 9). The total heat generated (Q_{gen}) is calculated according to the following equation:

$$Q_{gen} = Y m_{cal}(-\Delta H_{rxn}) \quad (9)$$

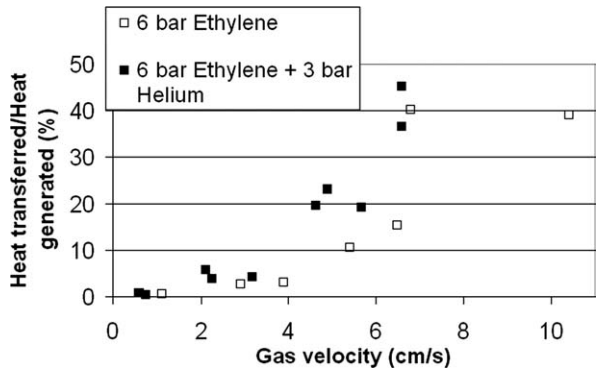

Figure 9. Efficiency of solid–gas heat transfer.

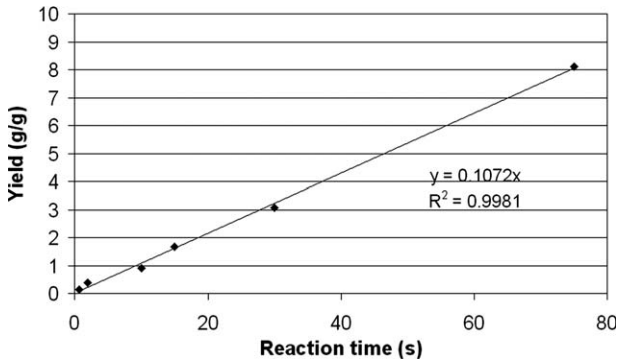

Figure 11. Yield dependence on reaction time (T = 80°C, P_{C2} = 6 bar, gas velocity = 3.0 cm/s, seedbed = NaCl coarse).

where Y is the yield, m_{cat} is the catalyst mass, and ΔH_{rxn} is the reaction enthalpy. The total heat transferred to the gas is calculated according to Eq. 6.

From Figure 9, it is clear that helium increases the quantity of heat transferred to the gas. In addition, as only a fraction of the heat is removed at low flow rates, it is important to recall that using helium at high flow rates can help reduce temperature excursions when the convective term is not preponderant. As the convective contribution to heat transfer becomes relevant, gas conductivity variations do not improve drastically the situation.

Simulations using a simple adiabatic model for the reactor allow us to estimate qualitatively the influence of the gas velocity and composition on heat removal from the solid particles and supporting the experimental observations shown above. The quantity of heat accumulated into the solid phase (Q_{solid}) is calculated from the difference between the values of Q_{gen} (Eq. 9) and Q_{gas} (Eq. 6). The solid phase is composed by the catalyst, the produced polymer, the inert seedbed, and the outlet steel frit (which has an estimated mass of 5 g). The outlet frit has to be put into the heat balance because the point at which the outlet gas temperature is measured is located beyond the frit itself. All the solids cited above are assumed to be under thermal equilibrium among each other.

Calculation of Q_{solid} for different reaction conditions allows estimating the solid temperature increase and its dependence on gas velocity and composition. The assumptions of the reactor being adiabatic and the solids being under thermal equilibrium are clearly not fully true but justified. They allow in fact a tremendous simplification of the calculations without affecting the trends of the results. The goal of these calculations being to obtain order of magnitude estimates of temperature changes supporting experimental observations shows that these assumptions are fully acceptable at this point.

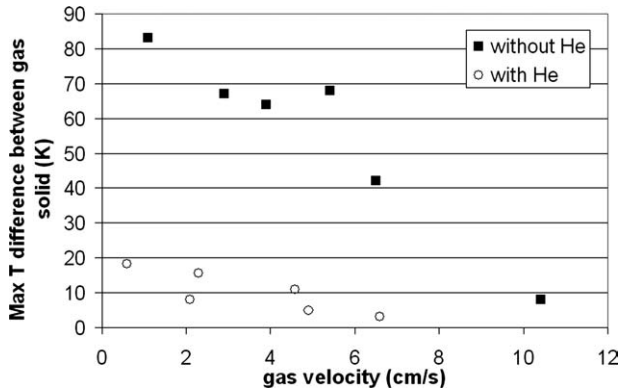

Figure 10. Calculated maximum T difference between the solid and the gas phases as a function of gas velocity and stream composition.

The series of experiments A and B presented previously in Figures 6–8 were ''simulated'' and results are summarized in Figure 10.

Constant catalyst activity has been supposed to perform the calculations. This is not so far from reality for these reaction conditions as can be seen from the measured linearity between yield and reaction time presented in Figure 11.

From Figure 10, it can be seen how the calculated increase of solid temperature can reach very high values leading to polymer melting (as seen in experiments) if no helium is added to the feed. Taken into account that gas temperatures can reach easily 100°C, values of 180°C has been estimated for the solid phase at low gas velocity. Only with gas velocities higher than 10 cm/s the solid heating is limited and melting is reduced. When helium is present in the gas feed (series B), the calculated solid temperature increase shows much lower values so that melting and thermal runaway are avoided as confirmed by experimental observations.

It is clear that increasing the gas velocity (no matter if helium is present or not in the feed) leads to an improvement in the heat transfer from the solid to the gas. The particle temperature is closer and closer to the measured outlet gas temperature as the gas velocity increases.

Influence of bed particle properties on heat transfer

The influence of the solid phase properties on heat transfer in packed bed has been studied for longtime.[49–54] From these studies, we can learn that decreasing the particle size improves the heat transfer from solid to gas because of the increase of the heat-transfer coefficient, whereas the solid thermal conductivity has a limited role in the overall rate of heat transfer in the bed.

Our case is slightly different from what is discussed in literature because the concentration of reacting particles is relatively

Table 2. Bed Particle Size Effect (T = 80°C, P_{C2} = 6 bar, reaction time = 75 s, m_{cat} = 30 mg)

Run	Bed Size (μm)	Yield (g/g)	Gas Velocity (cm/s)	Gas Max ΔT (K)	Time of Gas Max ΔT (s)	Heat Transferred to the Gas (%)
1	250–500	8.1	3.0	25	75	6
2	250–500	8.4	3.0	21	75	4
3	10–30	4.0	2.0	23	35	10
4	10–30	3.6	2.0	19	30	8

low here with respect to what one might encounter in a typical industrial process. In this section, we will investigate the role of the bed packing on the evolution of the outlet gas phase temperature. We can also neglect the impact of polymer production here as the expansion of the bed for the most productive run shown above is ~11%. This means that we can approximately represent our bed as a fixed bed heat exchanger with a heat source distributed homogeneously through the bed.

Varying the inert seedbed particle size will lead to differences in the flow field around the catalyst particles. Channeling or even by pass of the reacting particle by the gas[22] can be present leading to lower performances and reduced global activities. If an inert solid with too high particle diameter is used, it can happen that catalyst particles are placed ''behind'' (from the flowing gas point of view) an inert one. In this case, the reacting particle is shielded by the bigger one and its productivity is decreased.

As explained in the ''Experimental Part'' Section, the possibility to separate the formed polymer from the inert diluent by washing with water is a simple and elegant mean of operating if we can use NaCl as the dispersant.

To study the effect of the particle seedbed properties on heat transfer in start up of olefin polymerization in a packed bed, different reactions were performed using coarse NaCl or small NaCl as inert diluent (see the ''Experimental'' Section for details). Reaction conditions are shown in Table 2. It should be noted that the gas velocities are slightly different for the two inerts. All the experiments have been performed at the same gas volumetric flow rate (controllable parameter). The difference in gas velocity comes from the fact that the porosity of a bed of fine NaCl is much higher than that of coarse NaCl (0.40) because of the irregular and slightly agglomerated structure of the synthesized crystals.

Decreasing the seedbed particle size leads to an improved heat transfer in the bed: the gas peak temperature does not decrease considerably with seedbed particle diameter as the yield is reduced by a factor of 2 (Table 2). Smaller particles have a higher specific surface and more contact points so that convection to the fluid and especially conduction from catalyst to seedbed are improved. The last column of Table 2 tells us that the improvement in the heat transferred to the gas is not significant, but appears to be real. Varying the seedbed, particle diameter has in fact only a minor effect on the gas phase. Increasing the mean conduction of the solid phase has as consequence to accelerate the system dynamic response for heat transfer to the gas (as confirmed by T profiles of Figure 12).

Reactor heat-transfer optimization

Exploiting the effects explained above in synergy is the natural following step to have a tool allowing performing highly exothermic transient reactions without affecting the real kinetics or the particle morphology.

Figure 13 summarizes clearly what are the independent effects of each of the three variables that are in play:

- Gas conductivity (k_f): if increased, it improves heat transfer to the gas at low gas velocities avoiding catalyst overheating and thermal runaway.
- Gas velocity (V_g): if increased, it increases consistently the heat transfer to the gas and the dynamic response of the system.
- Seedbed particle size (D_p): if decreased, it increases mainly the bed average conductivity and the system dynamic response.

A judicious choice of the three parameters listed above leads to a significant improvement in the system performance (cfr Table 3 and Figure 13).

A gas velocity of 2.8 cm/s coupled with the presence of 33% molar helium in the feed and a small bed particle diameter (run 6 in Table 3) is sufficient to avoid thermal runaway (see yield column in Table 3) for our catalyst at 6 bars of ethylene and 80°C. It has to be noticed how reaction conditions of run 7 (gas velocity 5.5 cm/s, addition of 33 molar percent of helium and fine NaCl as seedbed) allow to remove 90% of the produced heat after a reaction of 75 s. Heat removal operating with the initial nonoptimized conditions (run 1) was of only 6%.

In column 6 of Table 3, it can be seen how an improvement of the heat transfer regime corresponds with an early apparition of the outlet gas temperature peak. This confirms that the reactor is now operating in a controlled way. It has to be said in fact (anticipating the following results) that catalyst activity in gas phase ethylene polymerization is 10 times higher at the very beginning of the reaction (first 2–5 s) than later. The rate of heat production follows this trend (Figure 14) so that a high gas temperature in the first seconds is to be expected with satisfactory heat transfer conditions.

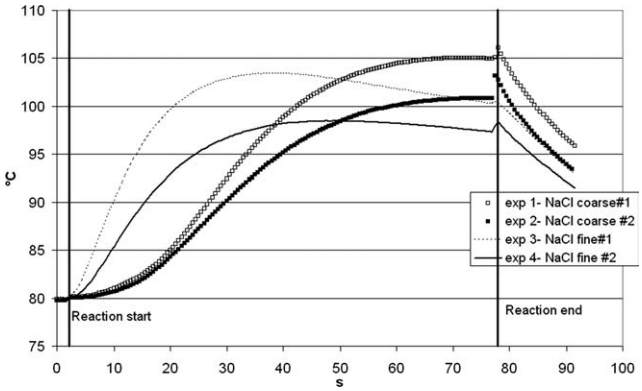

Figure 12. Bed particle size effect on outlet gas *T* profiles.

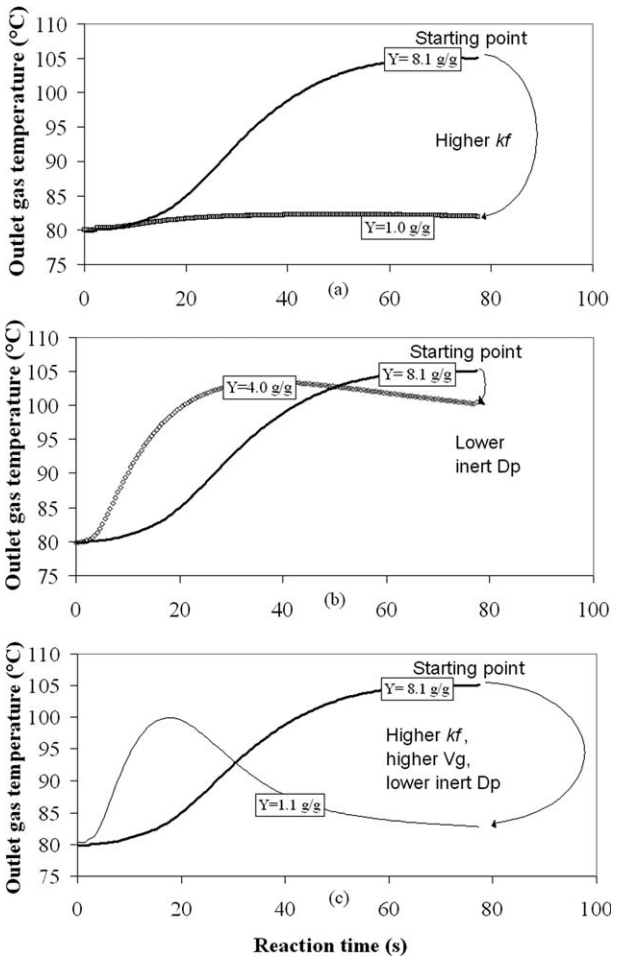

Figure 13. Summary of influence of the various parameters on activity and outlet stream temperature (T = 80°C, P_{C2} = 6 bar, reaction time = 75 s, m_{cat} = 30 mg).

(a) (—) (run 1) seedbed = NaCl coarse, gas velocity = 3.0 cm/s, 0 bar He; (□) (run 5) seedbed = NaCl coarse, gas velocity = 2.3 cm/s, 3 bar He. (b) (—) (run 1) seedbed = NaCl coarse, gas velocity = 3.0 cm/s, 0 bar He; (◇) (run 3) seedbed = NaCl small, gas velocity = 2.0 cm/s, 0 bar He. (c) (—) (run 1) seedbed = NaCl coarse, gas velocity = 3.0 cm/s, 0 bar He; (–) (run 7) seedbed = NaCl small, gas velocity = 5.5 cm/s, 3 bar He.

Nevertheless, it is not possible to observe an instantaneous appearance of the temperature peak of the outlet gas stream in this kind of reactor. This is because the heat produced at the active sites must diffuse through the catalytic particle to reach the surface (this is very rapid) and then it is evacuated either by leading to a local increase in the temperature of the neighboring bed particles or by being convected out of the reactor

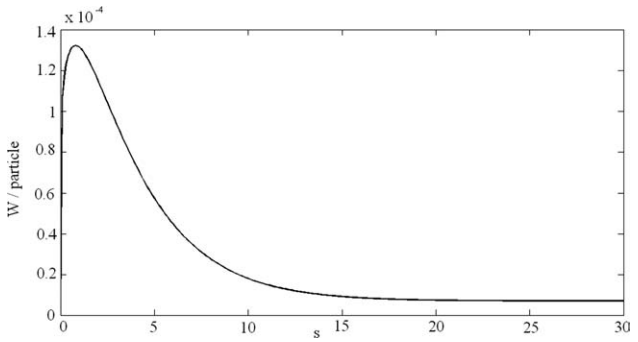

Figure 14. Calculated heat rate production (Watt per particle) from experimental activity data for run 6.

in the gas phase. It is likely that there is going to be a small but unavoidable time lag in establishing a high outlet gas temperature associated with heating of the bed material.

In Figure 15, the ratio of the instantaneous heat (power) removed by the gas to the power generated is plotted for experiments conducted at different reaction times. Each bar on the graph corresponds then to an experiment. Three series of experiments are shown: coarse NaCl as seedbed, no helium addition, 3 cm/s gas velocity (black bars); fine NaCl as seedbed, addition of 33 molar percent of helium to the feed, 5.5 cm/s gas velocity (stripy bar); and fine NaCl as seedbed, addition of 33 molar percent of helium to the feed, 15 cm/s gas velocity (crossed bars).

It is noticeable from this figure how for very short times (<2 s), no matter the reaction conditions, very little heat is absorbed by the gas phase. This supports the conclusions explained above. In addition it is easy to see how an improvement in heat transfer conditions increases not only the quantity of heat removed by the gas at "long" reaction times (30–75 s) but also allows a quicker removal thus lowering the probability for thermal runaway or for hotspots formation in the early instants of the polymerization. An instantaneous heat removal higher than 100% means that the flowing gas is capable both of evacuating all the heat produced and of cooling down the reacting bed. The sooner the instantaneous heat removal reaches these values, the sooner the bed starts to cool down and the less the probability to have bed overheating or melting and hotspots. Working with the original conditions (black bars) leads to an instantaneous heat removal of only 28% after 75 s of reaction: the bed is still heating up and is probably completely melted down. Working with the best conditions for heat transfer (crossed bars) leads to a heat removal of 150% after only 15 s: the bed heats up because of the produced heat reaching a maximum temperature between 4 and 15 s and then rapidly cools down. The shortness of the period during which the bed is

Table 3. Optimum Heat Transfer (T = 80°C, P_{C2} = 6 bar, reaction time = 75 s, m_{cat} = 30 mg)

Run	Bed Size (μm)	Helium (bar)	Gas Velocity (cm/s)	Gas Max ΔT (K)	Time of Gas Max ΔT (s)	Efficiency (%)	Yield (g/g)
1	250–500	0	3.0	25	75	6	8.1
3	10–30	0	2.0	23	35	10	4.0
5	250–500	3	2.3	2.3	45	8	1.0
6	10–30	3	2.8	17	15	33	1.3
7	10–30	3	5.5	20	15	90	1.1

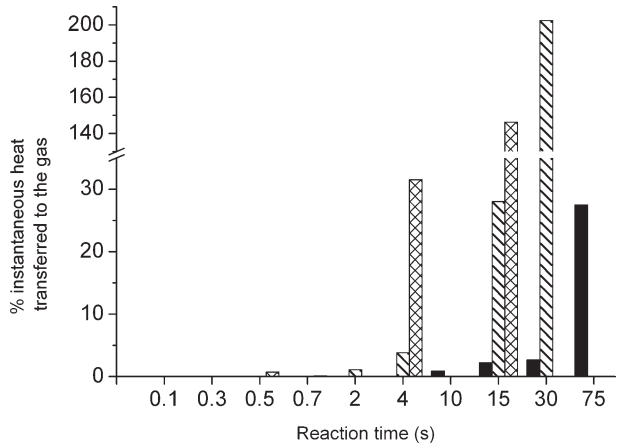

Figure 15. Amount of heat transferred to the gas at different reaction times ($T = 80^{\circ}C$, $P_{C2} = 6$ bar).

heating up decreases the probability to have reached too high temperatures. These two opposite situations explain the sensitivity of this reacting system (catalyst and reactor) to heat transfer and its influence on catalyst activity.

Finally, a percentage of heat transferred to the gas reaching high values very soon can be translated into a fast increase of gas temperature and an early apparition of the maximum. The outlet gas temperature profile is then closer to the heat rate production profile (Figure 14) and, as a consequence, particle surface and gas temperatures are close each other all along the duration of the reaction.

Conclusions

A study of heat transfer in a packed-bed reactor for short time gas phase olefin polymerization has been presented. The influence of gas and solid (seedbed) physical parameters has been studied so as their synergic effects. It has been demonstrated that enhanced gas conductivity by helium addition to the feed, high enough gas flow rate and small size of the inert seedbeds (comparable to catalyst particle) are fundamental characteristics to operate in a controlled way. It has been shown how in this original equipment heat transfer optimization is quite challenging due to the reduced possibilities for the heat to be removed and delicate due to the necessity to obtain enough polymer for analysis. It has been shown how there is a strong relation between heat transfer quality and measured catalyst activity in short time reaction. This can vary by a factor of 7 only by changing some process physical parameters. It is then clear that an optimization of the reaction conditions is fundamental to avoid falsified kinetics and catalyst deactivation or even polymer melting into the catalyst pores. In addition, all the work done here can be a strong basis for the building of a transient state calorimetric model of the reactor and for the measurements of the catalyst particle temperature during the start-up of a gas phase catalytic olefin polymerization.

Acknowledgments

Financial support by Dutch Polymer Institute is gratefully acknowledged. This work is part of the Research Programme of the Dutch Polymer Institute (DPI, Eindhoven, The Netherlands), project nr. #636. R.S. is also indebted to ANR (project ANR-06-BLAN-0269).

Literature Cited

1. Chum PS, Swogger KW. Olefin polymer technologies—history and recent progress at the Dow Chemical Company. *Prog Polym Sci*. 2008;8:797–819.
2. McKenna TFL, Soares JBP. Single particle modelling for polyolefins: a review. *Chem Eng Sci*. 2001;56:3931–3949.
3. McKenna TFL, Di Martino A, Weickert G, Soares JBP. Particle growth during the polymerisation of olefins on supported catalysts. 1. Nascent polymer structures. *Macromol React Eng*. 2010;4:40–64.
4. Song F, Cannon RD, Bochmann M. Zirconocene-catalyzed propene polymerization: a quenched-flow kinetic study. *J Am Chem Soc*. 2003;125:7641–7653.
5. Busico V, Cipullo R, Esposito V. Stopped-flow polymerizations of ethene and propene in the presence of the catalyst system *rac*-Me_2Si(2-methyl-4-phenyl-1-indenyl)$_2ZrCl_2$/methylaluminoxane. *Macromol Rapid Commun*. 1999;20:116–121.
6. Liu B, Matsuoka H, Terano M. Stopped-flow techniques in Ziegler catalysis. *Macromol Rapid Commun*. 2001;22:1–24.
7. Fink G, Tesche B, Korber F, Knoke S. The particle forming process of SiO_2-supported metallocene catalysts. *Macromol Symp*. 2001; 173:77–87.
8. Di Martino A, Broyer JP, Scweich D, De Bellefon C, Weickert G, McKenna TFL. Design and implementation of a novel quench flow reactor for the study of nascent olefin polymerisation. *Macromol React Eng*. 2007;1:284–294.
9. Di Martino A, Weickert G, McKenna TFL. Contributions to the experimental investigation of the nascent polymerisation of ethylene on supported catalysts. 1. A quenched-flow apparatus for the study of particle morphology and nascent polymer properties. *Macromol React Eng*. 2007;1:165–184.
10. Di Martino A, Weickert G, McKenna TFL. Contributions to the experimental investigation of the nascent polymerisation of ethylene on supported catalysts. 2. Influence of reaction conditions. *Macromol React Eng*. 2007;1:229–242.
11. Silva FM, Broyer JP, Novat C, Lima EL, Pinto JC, McKenna TFL. Investigation of catalyst fragmentation in gas-phase olefin polymerisation: a novel short stop reactor. *Macromol Rapid Commun*. 2005;26:1846–1853.
12. Jessup RS. The heat and free energy of polymerization of ethylene. *J Chem Phys*. 1948;16:661–664.
13. Floyd S, Choi KY, Taylor TW, Ray WH. Polymerization of olefins through heterogeneous catalysis. III. Polymer particle modelling with an analysis of intraparticle heat and mass transfer effects. *J Appl Polym Sci*. 1986;32:2935–2960.
14. Floyd S, Choi KY, Taylor TW, Ray WH. Polymerization of olefines through heterogeneous catalysis. IV. Modeling of heat and mass transfer resistance in the polymer particle boundary layer. *J of Appl Polym Sci*. 1986;31:2231–2256.
15. Yiagopoulos A, Yiannoulakis H, Dimos V, Kiparissides C. Heat and mass transfer phenomena during the early growth of a catalyst particle in gas-phase olefin polymerization: the effect of prepolymerization temperature and time. *Chem Eng Sci*. 2001;56:3979–3995.
16. Webb SW, Weist EL, Chiovetta MG, Laurence RL, Conner WC. Morphological influences in the gas phase polymerization of ethylene by silica supported chromium oxide catalysts. *Can J Chem Eng*. 1991;69:665–681.
17. McKenna TFL, Cokljat D, Wild P. CFD modelling of heat transfer during gas phase olefin polymerization. *Comput Chem Eng*. 1998; 22:285–292.
18. Ferrero MA, Chiovetta MG. Catalyst fragmentation during propylene polymerization, part I. The effects of grain size and structure. *Polym Eng Sci*. 1987;27:1436–1447.
19. Ferrero MA, Chiovetta MG. Catalyst fragmentation during propylene polymerization. III. Bulk polymerization process simulation. *Polym Eng Sci*. 1991;31:886–903.
20. Ferrero MA, Chiovetta MG. Effects of catalyst fragmentation during propylene polymerization. IV. Comparison between gas phase and bulk polymerization processes. *Polym Eng Sci*. 1991;31:904–911.
21. McKenna TFL, Spitz R, Cokljat D. Heat transfer from catalysts with computational fluid dynamics. *AIChE J*. 1999;45:2392–2410.
22. Eriksson EJG, McKenna TFL. Heat-transfer phenomena in gas-phase olefin polymerization using computational fluid dynamics. *Ind Eng Chem Res*. 2004;43:7251–7260.

23. Hamilton P, Hill DR, Luss D. Optical and infrared study of individual reacting metallocene catalyst particles. *AIChE J*. 2008;54:1054–1063.
24. Zacca JJ, Debling JA, Ray WH. Reactor residence time distribution effects on the multistage polymerization of olefins. I. Basic principles and illustrative examples, polypropylene. *Chem Eng Sci*. 1996; 51:4859–4886.
25. Pater JTM, Weickert G, Van Swaaij WPM. Optical and infrared imaging of growing polyolefin particles. *AIChE J*. 2003;49:450–464.
26. Keii T, Terano M, Kimura K, Ishii K. A kinetic argument for a quasi-living polymerization of propene with a $MgCl_2$-supported catalyst. *Makromol Chem Rapid Commun*. 1987;8:583–587.
27. Soga K, Ohgizawa M, Shiono T, Lee DH. Possibility of mass-transfer resistance in ethylene polymerization with magnesium chloride-supported catalysts. *Macromolecules*. 1991;24:1699–1700.
28. Soga K, Ohgizawa M, Shiono T. Copolymerization of ethylene and propene with a $TiCl_4/MgCl_2$-$Al(C_2H_5)_3$ catalyst system using a stopped-flow method. *Macromolecules*. 1993;194:2173–2181.
29. Olalla B, Broyer JP, McKenna TFL. Heat transfer and nascent polymerisation of olefins on supported catalysts. *Macromol Symp*. 2008; 271:1–7.
30. Tioni E, Broyer JP, Spitz R, Monteil V, McKenna TFL. Heat transfer in gas phase olefin polymerisation. *Macromol Symp*. 2009;285:58–63.
31. Wakao N. Particle-to-fluid transfer coefficients and fluid diffusivities at low flow rate in packed beds. *Chem Eng Sci*. 1976;31:1115–1122.
32. Dhingra SC, Gunn DJ, Narayanan PV. The analysis of heat transfer in fixed beds of particles at low and intermediate Reynolds numbers. *Int J Heat Mass Transfer*. 1984;27:2371–2385.
33. Gunn DJ, Narayanan PV. Particle-fluid heat transfer and dispersion in fluidised beds. *Chem Eng Sci*. 1981;36:1985–1995.
34. Wen D, Ding Y. Heat transfer of gas flow through a packed bed. *Chem Eng Sci*. 2006;61:3532–3542.
35. Shent J, Kaguei S, Wakao N. Measurements of particle-to-gas heat transfer coefficients from one-shot thermal responses in packed beds. *Chem Eng Sci*. 1981;36:1283–1286.
36. Dixon AG, Cresswell DL. Theoretical prediction of effective heat transfer parameters in packed beds. *AIChE J*. 1979;25:663–676.
37. Mears DE. Diagnostic criteria for heat transport limitations in fixed bed reactors. *J Catal*. 1971;20:127–131.
38. Romkes SJP, Dautzenberg FM, Van den Bleek CM, Calis HPA. CFD modeling and experimental validation of particle-to-fluid mass and heat transfer in a packed bed at very low channel to particle diameter ratio. *Chem Eng J*. 2003;96:3–13.
39. Gnielinski V. Gleichungen zur Berechnung des Wärme- and Stoffaustausches in durchströmten ruhenden Kugelschüttungen bei mittleren and grossen Pecletzahlen. Verfahrenstechnik. 1978;12:63–366.
40. Martin H. Low Peclet Number Particle-to-Fluid Heat and Mass Transfer in Packed Beds. *Chem. Eng. Sci*. 1978;33:913–919.
41. Bird RB, Stewart WE, Lightfoot EN. *Transport Phenomena*. New York: Wiley, 1960.
42. Wakao N, Kaguei S, Funazkri T. Effect of fluid dispersion coefficients on particle-to-fluid heat transfer coefficients in packed beds : Correlation of Nusselt numbers. *Chem Eng Sci*. 1979;34: 325–336.
43. Gunn DJ. Transfer of heat or mass to particles in fixed and fluidized beds. *Int J Heat Mass Transfer*. 1978;21:467–476.
44. Kittilsen P, McKenna TFL. Study of the kinetics, mass transfer, and particle morphology in the production of high-impact polypropylene. *J Appl Polym Sci*. 2001;82:1047–1060.
45. Zhou JM, Li NH, Bu NY, Lynch DT, Wanke SE. Gas-phase ethylene polymerization over polymer-supported metallocene catalysts. *J Appl Polym Sci*. 2003;90:1319–1330.
46. Gaillard C, Despois JF, Mortensen A. Processing of NaCl powders of controlled size and shape for the microstructural tailoring of aluminium foams. *Mater Sci Eng A*. 2004;374:250–262.
47. Perry RH, Green DW. *Perry's Chemical Engineer's Handbook*, 7th ed. New York: McGraw-Hill, 1997.
48. Poling BE, Prausntiz JM, O'Connel JP. *The Properties of Gases and Liquids*, 5th ed. New York: McGraw-Hill, 2004.
49. Wakao N, Kaguei S, Shiozawa B. Effect of axial fluid thermal dispersion coefficient on Nusselt numbers of dispersion-concentric model of packed beds at low flow rates. *Chem Eng Sci*. 1977; 32:451–454.
50. Pereira Duarte SI, Barreto GF, Lemcoff NO. Comparison of two-dimensional models for fixed bed catalytic reactors. *Chem Eng Sci*. 1984;39:1017–1024.
51. Pereira Duarte SI, Ferretti OA, Lemcoff NO. A heterogeneous one-dimensional model for non-adiabatic fixed bed catalytic reactors. *Chem Eng Sci*. 1984;39:1025–1031.
52. Martinez OM, Pereira Duarte SI, Lemcoff NO. Modeling of fixed bed catalytic reactors. *Comput Chem Eng*. 1985;9:535–545.
53. Andrigo P, Bagatin R, Pagani G. Fixed bed reactors. *Catal Today*. 1999;52:197–221.
54. Vortmeyer D, Schaefer RJ. Equivalence of one- and two-phase models for heat transfer processes in packed beds: one dimensional theory. *Chem Eng Sci*. 1974;29:485–491.

Manuscript received Nov. 23, 2010, and revision received Jan. 17, 2011.